

ROBUST AUTOPILOT DESIGN USING μ -SYNTHESIS

R.T. Reichert
Senior Engineer
The Johns Hopkins University Applied Physics Laboratory
Laurel, Maryland

ABSTRACT

This paper examines the applicability of H_∞ and μ -synthesis control to the design of automatic flight control systems for highly maneuverable, tail-controlled missiles. The impact on performance, of the degree of conservatism inherent to each approach, is examined. It is shown that μ -synthesis provides a superior framework for the design of missile autopilots which exhibit robust performance.

INTRODUCTION

Future homing missiles will need to cope with demands for greater range and higher maneuverability resulting in more stringent autopilot performance requirements. Design techniques, used in current practice, are limited and often result in less capable system performance. However, recent advances in robust-control theory [1-4] offer good prospects for meeting the design needs of next generation missiles. Several anticipated benefits of the robust-control design approach are: greater flexibility in the choice of airframe geometry, full use of available airframe maneuver capability and greater tolerance to uncertainty in design models.

Robust-control design methods optimize performance and stability based on engineering models which include performance specifications and descriptions of how uncertainty modifies the nominal plant model. H_∞ optimal control provides the basis for controller synthesis while μ -analysis characterizes performance and stability in the presence of a defined structure for uncertainties. The combination of these two powerful techniques leads to μ -synthesis. This paper focuses on showing the differences between H_∞ optimal control, which, by itself ignores the structure of uncertainty, and μ -synthesis.

ANALYSIS REVIEW

Definition: Linear Fractional Transformation (LFT). Consider the complex matrix partitioned as

$$M = \begin{bmatrix} M_{11} & M_{12} \\ M_{21} & M_{22} \end{bmatrix}$$

derived from the following linear equations

$$\begin{bmatrix} z \\ e \end{bmatrix} = M \begin{bmatrix} w \\ v \end{bmatrix}$$

$$w = \Delta z$$

where the size of Δ is such that $M_{11}\Delta$ is square. This set of equations is well posed if the inverse of $I - M_{11}\Delta$ exists, in which case the vectors e and v will satisfy $e = F_u(M, \Delta)v$ where

$$F_u(M, \Delta) = M_{22} + M_{21}\Delta(I - M_{11}\Delta)^{-1}M_{12}.$$

If viewed in a feedback block-diagram sense, the notation used here denotes the LFT formed by closing the upper loop (hence, subscript u) of M with Δ . M_{22} may be viewed as a nominal element and Δ as a linear-fractional uncertainty. The matrices M_{11} , M_{12} , M_{21} and $F_u(M, \Delta)$ describe how Δ affects the nominal element.

The framework for analysis and synthesis, used here, is based on LFT's as shown in Figure 1. Any linear interconnection of inputs (v, u), outputs (e, y) and uncertainties (Δ) may be rearranged as shown in Figure 1a. P represents the system interconnection structure, K the controller and Δ the uncertainty. v is a vector of exogenous inputs such as reference commands, disturbances and noise. e is a vector of error signals to be kept small. y is a vector of sensor measurements and u is a vector of control signals. The convention adopted here is to normalize exogenous inputs (v), errors (e) and uncertainty (Δ) to 1. This requires that all scalings be absorbed into P .

Figure 1a. General Structure

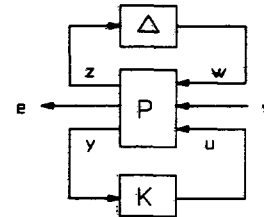


Figure 1b. Analysis

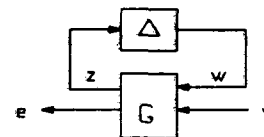
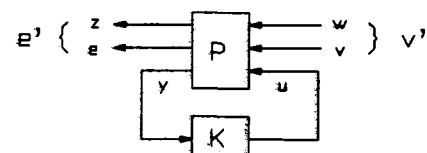


Figure 1c. Synthesis



Within this framework we will be concerned with 2 LFT structures; one for analysis (Figure 1b):

$$F_u(G, \Delta) = G_{22} + G_{21} \Delta (I - G_{11} \Delta)^{-1} G_{12},$$

where G is obtained by absorbing the controller K into P , and one for synthesis (Figure 1c):

$$F_1(P, K) = P_{11} + P_{12} \Delta (I - P_{22} \Delta)^{-1} P_{21}.$$

In the absence of uncertainty the nominal performance measure is given by

$$\|G_{22}\|_{\infty} = \sup_{\omega} \bar{\sigma}(G_{22}(j\omega)),$$

and relates the worst-case response, over frequency, to the exogenous input. Nominal stability, a weak requirement, is attained by K stabilizing only the nominal plant.

When uncertainty is considered, the analysis problem involves: determining the robust stability of G in the presence of an uncertain but bounded set of Δ 's, and for robust performance, determining if e remains in a desired set of responses for all permissible sets of Δ and exogenous inputs v . Stability for unstructured uncertainty (only $\bar{\sigma}(\Delta) \leq 1$ is known) depends only on $\|G_{11}\|_{\infty} \leq 1$, and performance depends only on $\|G\|_{\infty}$. However, norm bounds of this type are inadequate for determining robust performance or stability with realistic models of structured uncertainty in the plant. The structured singular value (μ) was introduced to deal with these more complicated situations [5].

In defining μ , we begin by specifying that Δ belongs to the set of block-diagonal, complex-valued, bounded uncertainties:

$$\Delta = \text{diag}(\Delta_1, \Delta_2, \dots, \Delta_n) \mid \bar{\sigma}(\Delta_i) \leq 1.$$

For $M \in \mathbb{C}^{n \times n}$, $\mu(M)$ is defined:

$$\mu(M) = \frac{1}{\min(\bar{\sigma}(\Delta) \mid \Delta \in \underline{\Delta}, \det(I - M\Delta) = 0)}$$

unless no $\Delta \in \underline{\Delta}$ makes $I - M\Delta$ singular, in which case $\mu(M) = 0$. The function μ is dependent upon the structure of Δ and has the property $\mu(\alpha M) = |\alpha| \mu(M)$.

The following bounds, which are relatively easier to compute, are defined for μ :

$$\sup_{U \in \underline{U}} \rho(MU) \leq \mu(M) \leq \inf_{D \in \underline{D}} \bar{\sigma}(DM D^{-1})$$

where

ρ denotes spectral radius
 $\bar{\sigma}$ denotes maximum singular value

$$\underline{U} = (\text{diag}(U_1, U_2, \dots, U_n) \mid U_i^* U_i = I)$$

$$\underline{D} = (\text{diag}(d_1 I, d_2 I, \dots, d_n I) \mid d_i \in \mathbb{R}_+)$$

where the structures of \underline{U} and \underline{D} match Δ . Note that \underline{U} and \underline{D} leave Δ invariant:

$$\bar{\sigma}(\Delta U) = \bar{\sigma}(U \Delta) \text{ and } D^{-1} \Delta D = \Delta.$$

The following two theorems [6] establish the relevance of μ for studying robustness of feedback systems with structured uncertainty.

Theorem: Robust Stability

$$F_u(G, \Delta) \text{ stable } \forall \Delta \in \underline{\Delta} \text{ iff } \sup_{\omega} \mu(G_{11}(j\omega)) \leq 1.$$

Theorem: Robust Performance

$$F_u(G, \Delta) \text{ stable and } \|F_u(G, \Delta)\|_{\infty} \leq 1$$

$$\forall \Delta \in \{\text{diag}(\Delta, \Delta_{n+1})\} \text{ iff } \sup_{\omega} \mu(G(j\omega)) \leq 1.$$

SYNTHESIS REVIEW

For synthesis it is assumed that performance weightings and scaling factors are absorbed as part of the interconnection structure (P in Figure 1.c) so that v' and e' are properly normalized to 1. For the H_{∞} optimal-performance problem the synthesis goal is to find a stabilizing controller K which minimizes $\|F_1(P, K)\|_{\infty}$ where

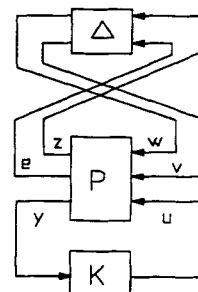
$$e' = F_1(P, K) v' \\ F_1(P, K) = P_{11} + P_{12} \Delta (I - P_{22} \Delta)^{-1} P_{21}.$$

A detailed review of H_{∞} control is given in [7] and state-space synthesis approaches, followed herein, are discussed in [1,2].

The H_{∞} optimal-performance problem posed here may be viewed as an H_{∞} robust-stabilization problem with respect to the uncertainty structure shown in Figure 2. Here Δ is considered to be a full-block of unstructured uncertainty (only $\bar{\sigma}(\Delta) \leq 1$ is known). That is, find K to stabilize the system and to minimize:

$$\|F_u(F_1(P, K), \Delta)\|_{\infty} \quad \forall \Delta \mid \bar{\sigma}(\Delta) \leq 1.$$

Figure 2. H_{∞} Robust Stabilization



Clearly, this represents a more conservative synthesis problem than is intended, because the true structure of Δ is ignored. In reality, Δ in Figure 2, has a structure dictated by the true uncertainty (which we denote $\Delta_u \mid \Delta_u \in \underline{\Delta}$) and a full-block structure for the e/v transfer function (which we denote Δ_p). This yields an actual structure for Δ , in Figure 2, of:

$$\Delta = \begin{bmatrix} \Delta_u & 0 \\ 0 & \Delta_p \end{bmatrix}$$

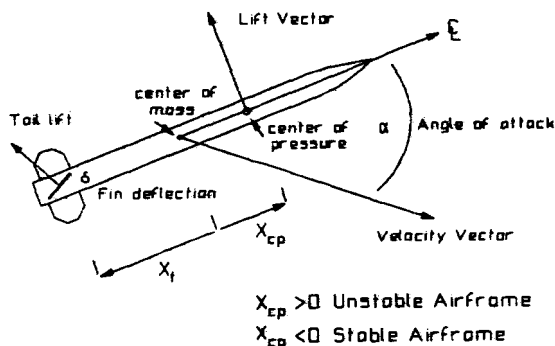
It should be noted that an H_∞ controller could be obtained without regard to the presence of internal modeling uncertainties (i.e., by removing the exogenous inputs and errors associated with the uncertain elements). This step removes all conservatism by assuming that the design model is a perfect representation of the plant response. The resulting design will surely exhibit very poor robust performance and stability in the presence of the real plant model.

In order to reduce conservatism, without removing it altogether, we will need to merge the two powerful techniques of H_∞ optimization and μ -analysis. Recall that an upper bound for μ may be obtained by a scaling operation and application of the $\| \cdot \|_\infty$. Incorporating this μ related concept with H_∞ synthesis, the problem becomes one of finding a controller K and a frequency dependent scaling matrix $D(s)$ such that $\|D(s)F_1(P,K)D(s)^{-1}\|_\infty$ is minimized. The approach taken here is to alternate between finding K , to minimize the above expression for a fixed $D(s)$, and then to find a minimizing $D(s)$ for a fixed K . This latter step is conducted point-by-point in frequency with a different constant D matrix result for each frequency point. The data for the elements of D may be fit with real-rational, minimum-phase, stable and invertible SISO transfer functions. The frequency dependent matrix $D(s)$ is comprised of the SISO transfer function fits. This μ -synthesis technique (D-K iteration) has been used extensively elsewhere to obtain robust control laws. The performance and robustness characteristics of the less conservative μ -synthesis approach will be compared with those obtained from the more conservative H_∞ -synthesis approach in the following sections.

PROBLEM DESCRIPTION

Consider the missile-airframe control problem illustrated in Figure 3. When the vehicle is flying with an angle of attack (α), lift is developed. This lift may be represented as acting at a central location (center of pressure). The vehicle will be statically stable or unstable (without corrective tail deflections) depending on the location of the center of pressure relative to the center of mass. The control problem requires that the autopilot generate the required tail-deflection (δ) to produce an angle of attack, corresponding to a maneuver called for by the guidance law, while stabilizing the airframe rotational motion.

Figure 3. Tail-Controlled Missile Problem



Sensor measurements for feedback typically include missile rotational rates (from rate gyros) and normal acceleration (from accelerometers). Reasonably accurate mathematical models of the rigid-body transfer functions from tail-deflection to the sensor outputs are generally available for design.

Typical uncertainties to be considered in this control problem include: aerodynamic characteristics, mass and balance, wind, flexible mode dynamics, actuator nonlinearities and sensor nonlinearities and noise. The first three uncertainties generally are handled by using sufficiently wide bandwidth feedback loops, while the last three uncertainties in the list act to restrict the amount of bandwidth that may be used practically.

For the problem considered here, it is desired to design one controller to track commanded acceleration maneuvers with a steady state accuracy of 0.5% and a time constant of less than 0.2 seconds. The controller must provide robust performance over a wide range of angles of attack and must avoid saturating tail-deflection actuator rate capabilities as well as avoid high-frequency instabilities caused by unmodelled flexible-body modes.

MISSILE MODEL

The nonlinear state equations for this control problem are given as:

$$\begin{aligned}\dot{\alpha} &= (\cos^2(\alpha)/m_u)[F_z] + q \\ \dot{q} &= M_y / I_y\end{aligned}$$

where

$$\begin{aligned}F_z &= C_z(\alpha, \delta) Q S \quad (\text{lbs}) \\ M_y^z &= C_m^z(\alpha, \delta) Q S d \quad (\text{ft-lbs}) \\ Q &= \text{dynamic pressure (lbs/ft}^2\text{)} \\ S &= \text{reference area (.44 ft}^2\text{)} \\ d &= \text{diameter (.75 ft)} \\ m &= \text{mass (13.98 slugs)} \\ I_y &= \text{pitch moment of inertia (182.5 slug-ft}^2\text{)} \\ u &= \text{velocity component along missile center line (3109.3 cos } \alpha \text{ ft/sec).}\end{aligned}$$

The aerodynamic coefficients C_z and C_m^z are given by the following polynomial expressions:

$$\begin{aligned}C_z &= a\alpha^3 + b\alpha^2 + c\alpha + d\delta \\ a &= .000103 \\ b &= -.00945 \\ c &= -.170 \\ d &= -.034 \\ C_m^z &= a\alpha^3 + b\alpha^2 + c\alpha + d\delta \\ a &= .000215 \\ b &= -.0195 \\ c &= .051 \\ d &= -.206\end{aligned}$$

These values are assumed to be representative of a missile travelling at Mach 3 at an altitude of 20,000 ft. The angle of attack is assumed to range over 0 to 20 degrees.

The nonlinear state equations are linearized about trim operating points ($M_y = 0$) to form linear state-space equations of the form:

$$\begin{aligned}\dot{x} &= Ax + Bu \\ y &= Cx + Du\end{aligned}$$

where $x = [\alpha \ q]$, $u = [\delta]$, and $y = [q \ \ddot{z}]$. Here, \ddot{z} represents the accelerometer measurement (assumed to be at the center of mass). For an angle of attack of 0 degrees, the state-space matrices are:

$$A = \begin{bmatrix} -0.6 & 1. \\ 32.4 & 0. \end{bmatrix}, \quad B = \begin{bmatrix} -.12 \\ -130.8 \end{bmatrix}$$

$$C = \begin{bmatrix} 0 & 1. \\ -1.02 & 0. \end{bmatrix}, \quad D = \begin{bmatrix} 0 \\ -.203 \end{bmatrix}$$

For an angle of attack of 20 degrees, the state-space matrices are:

$$A = \begin{bmatrix} -1.18 & 1. \\ -300.2 & 0. \end{bmatrix}, \quad B = \begin{bmatrix} -.11 \\ -130.8 \end{bmatrix}$$

$$C = \begin{bmatrix} 0 & 1. \\ -2.54 & 0. \end{bmatrix}, \quad D = \begin{bmatrix} 0 \\ -.203 \end{bmatrix}$$

As a representative average model to use in the design process we will select the following state-space matrices. These do not actually correspond to a given linearization about an operating angle of attack, rather they represent an average value for each element of the matrices when examined over the entire angle of attack range.

$$A = \begin{bmatrix} -0.9 & 1. \\ -134.0 & 0. \end{bmatrix}, \quad B = \begin{bmatrix} -.117 \\ -130.8 \end{bmatrix}$$

$$C = \begin{bmatrix} 0 & 1. \\ -1.78 & 0. \end{bmatrix}, \quad D = \begin{bmatrix} 0 \\ -.203 \end{bmatrix}$$

In addition to these dynamics, it is assumed that the missile tail-deflection actuator may be represented with a second order linear transfer function:

$$\frac{\delta}{\delta_c}(s) = \frac{1}{(s/\omega_a)^2 + (1.4s/\omega_a) + 1}$$

UNCERTAINTY DESCRIPTION

Three uncertainty descriptions will be used for this design example. The first captures the dominant effect of aerodynamic deviations from the assumed design model. The second represents uncertainty in the actuator gain and phase characteristics. And the last represents unmodelled dynamics. Figure 4 illustrates the location of the uncertain elements (Δ_1) in the design model.

The controller must handle the aerodynamic variations that result from operating over the angle of attack range from 0 to 20 degrees. Examining the state-space matrices over this range we see that the $A(2,1)$ element varies by as much as 140%. As expected, this term varies the most because it relates directly to the rotational stability of the rigid-body airframe. We will need to incorporate a parametric uncertain model to capture the uncertainty in this term. Variations in the other terms are known to far less significant, from physical considerations, and will be ignored. The normalizing scale factor for Δ_1 (k in Figure 4) for this example is 1.25. The effect of this uncertainty will be to make maximum use of the rate-gyro sensor for an inner-loop feedback path to desensitize the system from variations in the rotational aerodynamics.

The second uncertainty (Δ_2 in Figure 4) captures uncertainty in the actuator gain and phase characteristics. With a normalizing scale factor of $c=.6$, this uncertainty structure represents as much as 35 degrees phase uncertainty and gain variation from approximately .6 to 2.5). This uncertainty will have the effect of preserving gain and phase margin in the inner loop.

The third uncertainty (Δ_3 in Figure 4) is used to represent unmodelled flexible-mode dynamics. Figure 5 illustrates the frequency dependent weighting function $W_u(s)$ and a representative flexible mode transfer function from tail-deflection to rate-sensor measurement. The weighting functions represents a frequency dependent magnitude bound on the unmodelled transfer function. For conservativeness we elect to overbound the high frequency characteristics substantially. The effect of this uncertainty will be to limit the bandwidth available to the controller to handle aerodynamic variations.

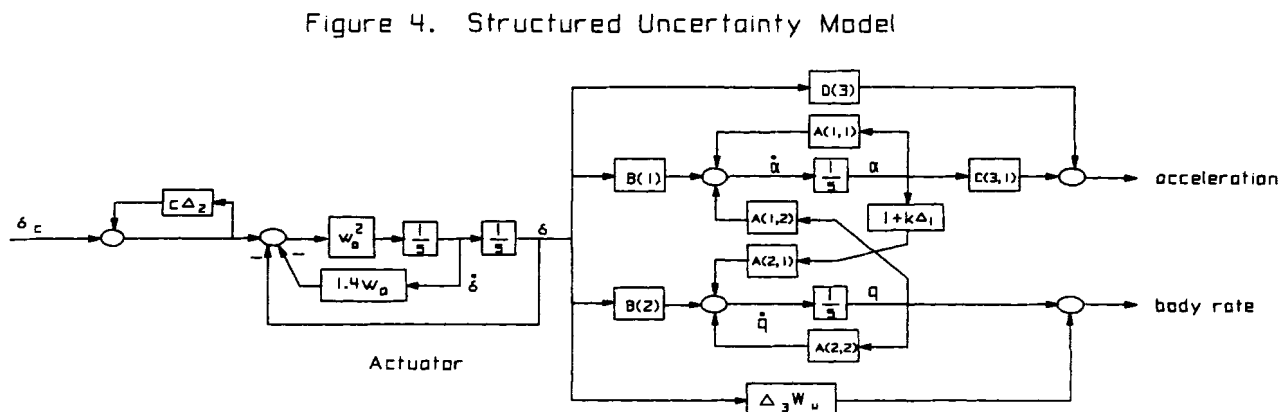
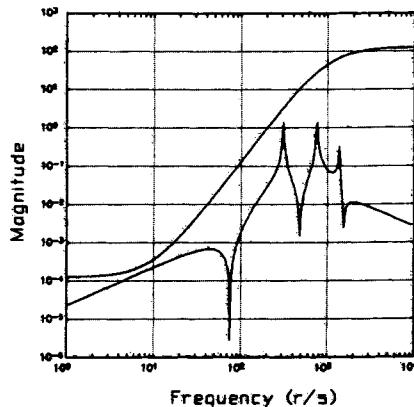


Figure 5. Unmodelled Flexible Mode Dynamics and Weighting Function



INTERCONNECTION STRUCTURE

Thus far, we have defined the nominal model of the plant and the uncertainty structure for this problem. The remaining portion of the interconnection structure to be defined is associated with the performance goals (i.e., exogenous inputs and errors associated with the tracking performance specifications). As stated earlier, the performance objective is to track step commands (η_c) with a 0.5% tracking accuracy and a maximum time constant of 0.2 seconds. To accomplish this we will define a frequency dependent weighting function that will be applied to the tracking error signal ($\eta_c - \eta$) (i.e., a sensitivity weighting function):

$$W_S(s) = \frac{(14.9451 s + 200)}{(42.7003 s + 1)}$$

This weighting function has a low frequency gain of 200 (For 0.5% tracking accuracy) a gain crossover frequency of 5 r/s (for 0.2 sec time constant or better) and a high frequency gain of 0.35 to limit overshoot.

The last exogenous input to be defined is the rate-gyro sensor noise. For this problem it is assumed that the gyro is a nearly perfect device. A scale factor of .001 is applied to this input. In practice, if realistic gyro characteristics were available, a frequency dependent weighting would be appropriate to characterize the anticipated noise spectrum.

COMPARISON OF H_∞ and μ -SYNTHESIS DESIGNS

For the interconnection structure defined here, the software provided in [8] was used to perform the D-K iteration for the μ -synthesis design. For the first step of the D-K iteration, the frequency dependent D-scale matrices were initialized to identities of the appropriate sizes. The resulting controller from this first pass is the H_∞ optimal controller (i.e., the controller designed with respect to the conservative model of Δ in Figure 2). For the first pass the performance level of $\|F_1(P,K)\|_\infty = 2.0$ was attained. For the final D-K iteration the robust-performance level $\|D(s) F_1(P,K) D(s)^{-1}\|_\infty = 1.07$ was achieved.

For evaluation purposes the H_∞ controller was reduced from 8th order to 7th and the μ controller was reduced from 20th order to 8th, using a balanced truncation model reduction procedure [9].

Figure 6 illustrates the step response performance characteristics of the H_∞ controller for the design model, and for the model linearized at two angles of attack (0 and 20 degrees). Figure 7 illustrates the μ -synthesis performance for the same three plant models. Clearly, the

Figure 6. H_∞ Design Responses

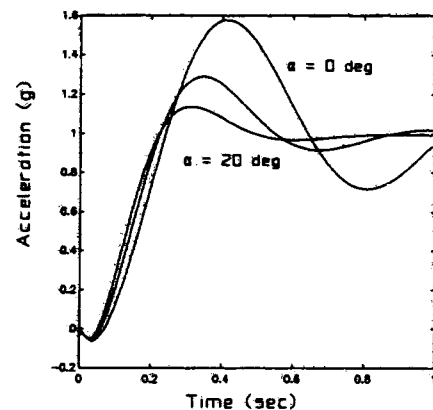
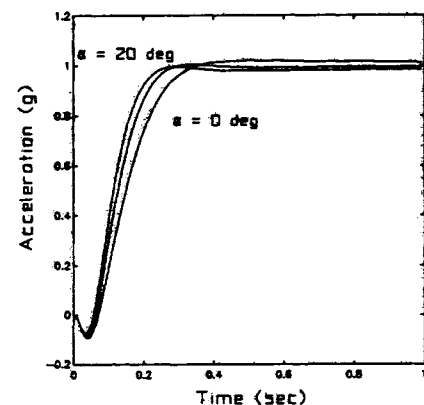


Figure 7. μ Design Responses



μ -synthesis controller exhibits superior tracking performance. Not shown here is that both designs satisfy the goal of gain stabilizing the unmodelled flexible-mode dynamics and that single-loop stability margins are very good (better than 6db and 35 degrees at the actuator input and at the sensor outputs).

Comparing the worst case perturbation matrices for the H_∞ and μ designs:

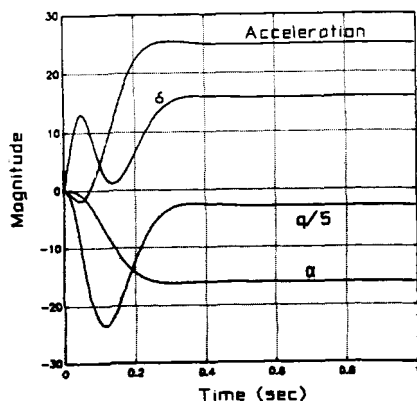
$$H_\infty \Rightarrow \begin{bmatrix} 0.0990 & -0.3416 & -0.2049 & -0.1384 \\ 0 & 0 & 0 & 0 \\ 0.0057 & -0.0195 & -0.0117 & -0.0079 \\ -0.0568 & 0.1959 & 0.1176 & 0.0794 \\ 0 & 0 & 0 & 0 \end{bmatrix}$$

$$\mu \Rightarrow \begin{bmatrix} 0.9346 & 0 & 0 & 0 \\ 0 & 0.9346 & 0 & 0 \\ 0 & 0 & -0.9346 & 0 \\ 0 & 0 & 0 & 0.9346 \\ 0 & 0 & 0 & .001 \end{bmatrix}$$

shows how the full-block uncertainty structure assumed in the H_∞ synthesis allows interaction between the various uncertainty structures and the performance inputs and outputs. Allowing this interaction presents a much more conservative design challenge and consequently the H_∞ design was unable to attain acceptable performance. It should be noted that only the real part of the worst-case uncertainties are shown above, however, in this case the imaginary parts were negligible.

As a final check on performance of the μ controller, a nonlinear simulation response of the system is shown in Figure 8. The autopilot was commanded to develop a 25g acceleration response, and as expected the controller performs very well.

Figure 8. Nonlinear Simulation Response



SUMMARY

Design for robust performance and stability requires, at a minimum, that the designer:

1. define a nominal model of the plant to be controlled,
2. define an uncertainty structure to characterize a family of plants in which it is anticipated that the real plant resides, and
3. express performance goals with normalized exogenous inputs and frequency weighted errors.

Use of a synthesis procedure, such as μ -synthesis, which preserves the structural relationship between uncertainties and performance elements, in the interconnect structure, is essential. Failure to account for this structured relationship may lead to overly conservative specifications and poor designs.

REFERENCES

1. J.C. Doyle, K. Glover, P. Khargonekar and B.A. Francis, "State-space Solutions to Standard H_2 and H_∞ Control Problems," ACC, Atlanta, GA, June 1988.
2. K. Glover, and J.C. Doyle, "State Space Formula for all Stabilizing Controllers that Satisfy an H_∞ Norm Bound and Relations to Risk Sensitivity", Systems and Control Letters, Vol 11, 1988.
3. G. Stein, "Beyond Singular Values and Loop Shapes," to appear AIAA Journal of Guidance and Control.
4. M. Safonov, and D. Limebeer, "Simplifying the H_∞ Theory via Loop Shifting," IEEE CDC Proceedings, 1988.
5. J.C. Doyle, "Performance and Robustness Analysis for Structured Uncertainty," IEEE CDC Proceedings, 1982.
6. J.C. Doyle, "Structured Uncertainty in Control System Design," IEEE CDC Proceedings, 1985.
7. B.A. Francis, "A course in H_∞ Control Theory," Springer-Verlag, Berlin, 1987.
8. "MUSYN Robust Control Short Course Notes and Software," September 1989, Arcadia CA.
9. R.Y. Chiang, and M.G. Safonov, "Robust-Control Toolbox for use with MATLAB and the Control System Toolbox", The Mathworks Inc.